Title Page

***Classification*:**

***Major category*:** Biological sciences ***Minor category*:** Plant Biology

***Title*:** Divergent Metabolome and Proteome Suggest Functional Independence of Dual Phloem Transport Systems in Cucurbits

Authors: Baichen Zhang[a,1,2], Vladimir Tolstikov[b], Colin Turnbull[c], Leslie M. Hicks[d] and Oliver Fiehn[b]

Author Affiliations: a. Max-Planck-Institute of Molecular Plant Physiology, Department of Lothar Willmitzer, 14424 Potsdam, Germany; b. UC Davis Genome Center, 451 Health Sciences Drive, Davis, CA, 95616-8816, USA; c. Division of Biology, Imperial College London, London SW7 2AZ UK d. Donald Danforth Plant Science Center, 975 North Warson Road, St Louis, MO, USA [1] Current Address: same as d.

[2] Corresponding author

Author contributions: BZ and OF designed research; BZ, VT, and LMH performed research; BZ, VT, LMH, CT and OF analyzed data; and BZ, CT and LMH wrote the paper.

[2] ***Corresponding author*:** Baichen Zhang: Proteomics & Mass Spectrometry Facility, Donald Danforth Plant Science Center, 975 N Warson Road, St Louis, MO, 63132, USA. Email: bzhang@danforthcenter.org Tel: 1-314-587-1225 Fax: 1-314-587-1325

Manuscript information

Text pages: 17, Figures: 4. Table 1, Supporting information: 7.

Abbreviations:

RFOs: raffinose family oligosaccharides; DAB: decolorized aniline blue; CF5(6): 5(6)-Carboxyfluorescein; SE/CCC: sieve element and companion cell complex; FP: fascicular phloem; EFP: extrafascicular phloem

Abstract

Cucurbitaceous plants (cucurbits) have long been preferred models for studying phloem physiology. However, these species are unusual in that they possess two different phloem systems, one within the main vascular bundles (fascicular phloem; FP) and another scattered through stem and petiole cortex tissues (extrafascicular phloem; EFP). We have revisited the assumption that the sap released following shoot incision originates from the FP, and also investigated the long-standing question of why the sugar content of this sap is about thirty-fold less than predicted for requirements of photosynthate delivery. Video microscopy unexpectedly reveals that FP very quickly becomes blocked on cutting, whereas the extrafascicular phloem bleeds for extended periods. Thus, all cucurbit phloem sap studies to date have reported metabolite, protein and RNA composition and material transport in the relatively minor extrafascicular sieve tubes. Using tissue dissection and direct sampling of sieve tube contents, we show that FP in fact does contain up to 1 M sugars, in contrast to low millimolar levels in the EFP. Moreover, major phloem proteins in sieve tubes of FP differ from those that predominate in the extrafascicular sap, and include several previously uncharacterized proteins with little or no homology to databases. The overall compositional differences of the two phloem systems strongly indicate functional isolation. On this basis, we propose that the fascicular phloem is largely responsible for sugar transport whereas the extrafascicular phloem may function in signaling, defense and perhaps transport of other metabolites.

\body

Introduction

Phloem transport systems have been extensively researched over the past century, as they perform vital functions in plants, including distribution of photoassimilates, nutrients and signaling molecules to spatially separated organs (1). A predominant concept in phloem physiology is that of a unified interconnected transport conduit (2). Both the complexity of phloem tissue organization and complications arising from rapid wound responses hamper studies on intact plants and limit access to the transported sap of most plant species (3). However, cucurbitaceous species (cucurbits) are preferred models for phloem physiology due to both the ease of sampling phloem sap and the facile visualization of their large phloem sieve elements. The earliest work dates back to Fisher (4), with the original observations of cucurbit phloem exudation by Crafts (5, 6) and Eschrich (7). Unusual amongst higher plants, cucurbits have two spatially separated phloem systems: fascicular phloem (FP) (7), also known as bundle phloem(8, 9), contained within vascular bundles, and extrafascicular phloem (EFP) (5). The latter is distributed as scattered elements throughout the cortex, peripheral to the vascular bundles (5, 8), and both outside (ectocyclic sieve tubes) and inside (endocyclic) the ring of sclerenchyma (Refer to (10) for an excellent drawing).

Cucurbit phloem transport has several noteworthy characteristics. Although many plants load sucrose apoplastically into phloem either against a concentration gradient (11) or with no loading step observed (12), cucurbits have been proposed instead to employ a polymer trapping strategy (13). In this model, sucrose diffuses symplastically into intermediate cells, where it is converted into raffinose-family oligosaccharide sugars (RFOs). The RFOs remain in the sieve element/companion cell complex (SE/CCC) due to a combination of their increased molecular mass and the different plasmodesmal size exclusion limits between mesophyll–intermediary cell and intermediary cell–sieve element junctions (13).

However, several aspects of cucurbit phloem transport and the polymer trapping model remain unresolved. The first problem is that the total RFO sugar content in cucurbit phloem exudates is around 50-fold lower than predicted from photosynthetic

output and mass flow calculations (14) and from equivalent data on phloem of other species. In contrast, amino acid content of cucurbit phloem exudate is similar to other species (15). It has been widely assumed, sometimes implicitly, that cucurbit exudates derive largely or exclusively from the much more substantial FP system, with only minor contributions from the EFP (16). Many explanations have been advanced. One suggestion is that the low RFO concentration in exudates is due to dilution by surrounding cells or by xylem sap (17), but this can be discounted based on the magnitude of dilution required, and from the fact that amino acid levels are similar to other species (18). These controversies have recently been reviewed (19).

The second problem concerns the extensively studied phloem exudate proteins (20). The two dominant proteins, known as PP1 and PP2, are thought to be major constituents of so-called P-protein bodies visible in sieve elements (21, 22). Microscopy shows that upon wounding, proteins appear to seal sieve tubes and should immediately block phloem transport (22). Why rapid blockage does not occur has long been a mystery, as exudation continues for several minutes. However, immunocytochemical evidence indicates that PP1 and PP2 may be absent from or only weakly present in FP, whereas they are abundant in EFP (8, 23). Images from tissue printing were equivocal (24).

In a previous report, the summed sugar concentration in cucurbit phloem exudates was found to be below 30 mM (18), consistent with many published studies but far less than the typical 1 M sugar content required to satisfy requirements of the mass flow mechanism. Cucurbit phloem should have highly concentrated sugars (19), considering the sugar transport required to sustain the rapid growth of fruits (25). Therefore, we questioned the consensus interpretations of the origins of phloem exudates, and have revisited the systems using a combination of video microscopy and transport experiments, together with metabolite and proteome analysis. We show that cucurbit phloem exudates originate from extrafascicular phloem and not from fascicular phloem. The data reveal massively divergent metabolite and protein contents between exudates and fascicular phloem tissue, suggesting that cucurbits have evolved two spatially and functionally distinct phloem systems.

Results

Re-investigation of phloem exudation in cucurbits. Shoots of intact pumpkin plants (*Cucurbita maxima*) were placed under a dissection microscope. The exudation process from petioles and stems was observed immediately after cutting. Even without staining, fascicular phloem regions within the normal cucurbit bicollateral, vascular bundles were readily recognized by their darker green color and location on either side of xylem tissues (Fig. 1*A* and 1*B*) (26). Identification of FP was confirmed with decolorized aniline blue (DAB) staining of callose, which marked the sieve elements (Fig. 1*I*).

On cutting, the instantaneous onset of phloem exudation was too rapid to allow us to clearly discern the exudate origins. Sap immediately spread over much of the cut surface. Individual droplets were usually not visible, nor was it apparent whether large drops were emanating from FP or from other locations (Fig. 1*A* and Supporting Information: Video S1). However, by repeatedly removing the exudates with filter paper, it was observed that the flow decreased substantially over a period of around 1-5 minutes. It then became clear that the exudate droplets came largely or exclusively from EFP and not from FP (Fig. 1 *C–H*). The low resolution of the stereomicroscope impaired direct recognition of unstained extrafascicular sieve tubes. However, the pattern of exudate droplets emanating from the stem surface exactly matched the known distribution of cucurbit EFP strands, i.e., immediately surrounding vascular bundles, scattered through the cortex and both outside (ectocyclic) and inside (endocyclic) the ring of sclerenchyma (10). These observations were confirmed from the video record of this exudation (Supporting Information: Video S1), and by detailed scrutiny of time-series still images. Even though exudation slowed with time after cutting, the sites from which exudate emerged did not change. Careful mapping of the sites from which the sap emerges show that they are all coincident with EFP and none with FP.

We next compared exudation in three other cucurbits (*Cucumis sativus*, *Cucurbita pepo*, and *Citrullus lanatus*) widely used in phloem studies. Their behavior was identical: no exudates were seen from FP regions and patterns of exudation sites were in complete agreement with known EFP distribution.

Because symplastic trapping of an externally applied phloem tracer [5(6)-Carboxyfluorescein (CF5(6)), or its diacetate form] to phloem systems is well

documented (27, 28), we further assessed the origin of exudates in pumpkin by applying this tracer to two sites: the leaf surface and the petiole surface, in separate experiments (Supporting Information: Fig. S1). One to two hours after application of CF5(6) to leaves, petioles were cut and observed. Exudates, FP tissues, and EFP tissues were all heavily labeled with yellow-green fluorescence (Fig. 2*A*). After exhaustive exudation, labeled FP and EFP tissues were still visible (Fig. 2*B*). This demonstrates that both phloem systems can load and transport CF5(6), and that CF5(6) remains largely contained within the phloem. However, this experiment cannot distinguish whether the exudate was from FP or EFP or both. When stems more distant from CF5(6)-treated leaves were observed, only the FP was labeled, but not EFP. Small amounts of fluorescence, released from FP tissue immediately after cutting, were seen spreading onto otherwise unlabeled areas over the cut stem surface (Fig. 2*C*) but the exudate was largely unlabeled. This indicates slower transport in, or loading of tracers into EFP compared with the FP, and further suggests that most or all of the exudate does not originate from FP.

Tracer applied to petioles resulted in different labeling patterns, but again showed that the exudate is from EFP. After an overnight uptake and transport period, exudates from petiole cut surfaces were labeled with fluorescence (Fig. 2*D).* After removing the exudates once or twice, exudation slowed and smaller fluorescent droplets formed (Fig. 2*E)*. However, in contrast to leaf-feeding experiments, no FP tissue labeling was observed. Callose staining with DAB marked the FP sieve elements, and confirmed that exudation was not from FP (Fig. 2*F*). The selective labeling also suggests a lack of symplastic transport from EFP to FP. Taking all the labeling experiments together, none of the observations lends support to the idea that the exudate is from FP. In particular, when only stem FP is fluorescently labeled, the exudates are clearly not labeled.

The video and labeling experiments establish that cucurbit phloem exudates originate largely or exclusively from EFP, not from FP. In contrast to rapid, sustained exudation from EFP, FP becomes blocked almost immediately upon cutting. A small amount of FP sap from broken FP sieve elements may become mixed with phloem exudates immediately after cutting, but this does not continue. Therefore, the sampled exudate, after discarding the initial droplets, is essentially pure EFP sap.

Differences in metabolome composition between two phloem systems in pumpkin. The difference in exudation behavior between the two phloem systems indicated that the systems may be functionally distinct, something that has not previously been demonstrated in other species, even those with complex phloem anatomy. A rapid sealing mechanism hampers sampling of FP sap, so we instead separately dissected external and internal FP tissues from lyophilized stem segments to estimate FP sap composition (Supporting Information: Fig. S2). For EFP sap composition, we used phloem exudates. In previous reports (18, 29), the metabolome of cucurbit phloem exudates was found to contain amino acids and secondary metabolites at concentrations similar to phloem of other plants. However, many of the amino acids and secondary metabolites present in phloem exudates are not detectable or are at trace levels in FP tissues (Fig. 3).

The majority of small compounds detected by GC/MS (mostly below 500 Da) in phloem exudates are either missing or at much lower concentrations in profiles of FP tissues [Fig. 3 *A–C*; for a list of compounds in phloem exudates, refer to (18)]. The dominant metabolites detected by GC/MS in dissected FP tissues are sucrose and raffinose. Stachyose and verbascose are too large to be detected by GC/MS, but were found by LC/MS (Fig. 3*D, 3E*). Similarly, LC/MS reveals that other compounds present in exudates, including two families of glycans and various secondary metabolites (refer to (29) for elucidated structures), are absent from or minimally present in dissected FP (Fig. 3 *D–F*). By far the most dominant metabolites in FP are therefore RFOs.

To estimate RFO concentrations in dissected tissues, we calculated the tissue volume and determined the proportion occupied by sieve elements through microscopic measurement. In the entire dissected external and internal FP tissues, the RFO sugar concentration exceeds 500 mM. Based on total sugars measured from leaf tissue, 15 mM of summed RFOs was estimated for phloem parenchyma. Approximately 45% of the phloem tissue volume was sieve elements and companion cell complexes (SE/CCC). From these numbers, FP sap was calculated to contain around 1 M total RFOs, mainly as stachyose, in contrast to 29 mM RFOs in phloem exudates. Of the five sample types analyzed (leaf disc, phloem exudates, xylem tissue, and external and internal FP tissues), only the FP contains high concentrations of RFOs (Table 1).

Differences in proteomes between two phloem systems. The preceding discoveries suggested that the proteomes of the two phloem systems might also differ. One important question was whether the major P-proteins present in exudates are also components of the P-protein bodies that block FP.

Proteins were sampled as aggregates from unfixed, live FP (Supporting Information: Fig. S3), and from extracted, dissected FP tissues. These proteins were separated alongside exudate samples by 1D SDS-PAGE to compare the protein profiles from both phloem systems. The well-defined P-proteins (PP1 and PP2) in EFP exudates appear to be absent in the FP (Fig. 4). Instead, at least five major protein bands were seen in FP samples. Additional proteins may be present, but their abundances were too low to be identified. Two-dimensional-PAGE analysis similarly showed five groups of FP proteins. We designated them as groups because each share similar masses and only show a horizontal shift in the IEF dimension of the 2D-gel. None of these groups is dominant in 2D-PAGE of phloem exudates (Supporting Information: Fig. S4*A* and S4*B*). Likewise, the major phloem exudate proteins detected on either 1D or 2D gels are not prominent in FP samples. The smearing in 1D gels of FP proteins is suggestive of extensive post-translational modifications, which was confirmed by 2D gel analysis (Fig. 4*B*). One group of FP proteins (66 kDa, as judged from 2D-gel) was detected as phosphorylated by phospho-staining (Supporting Information: Fig. S4*C* and S4*D*)

MASCOT searches of LC/MS peptide spectra confirmed that PP1 and PP2 are the dominant proteins in exudate samples and are not detected from FP samples. Searching of the NCBInr database returned no significant hits for any of the FP proteins analyzed from gel spots. However, the recently released cucumber genome (30) and pumpkin phloem sap proteome (31), together with translated cucurbit EST and Unigene databases (www.icugi.org), contained significant hits to *de novo* sequenced peptides from one of the most abundant proteins (designated as CmFPP1, for *C. maxima* Fascicular Phloem Protein, ~80 kDa; Fig. 4 and Supporting Information: Table S1). However, all other peptides from FP samples lack homology to any proteins previously reported in phloem exudates or, for that matter, in any tissue from any organism. Thus, the FP proteome represents a newly identified functional system within cucurbits that is distinct from the extensively studied proteome of phloem exudates. The horizontal protein spot series in

2D gels of FP proteins were confirmed to be isoforms by manual examination of MS/MS spectra. Full length sequences have yet to be obtained for these novel proteins, and there are further unidentified minor proteins visible on the gels.

Discussion

Dual phloem transport systems. By carefully revisiting the question of the origin of cucurbit phloem exudates and by comparing the metabolite and protein contents of both cucurbit phloem systems, we have established that cucurbit phloem sap samples obtained by standard exudation methods following tissue cutting represent primarily or exclusively the contents of EFP and not the major FP system. This is an unexpected result because there is a large body of literature on metabolites, hormones, proteins and RNA in cucurbit phloem exudates resting on the assumption that cucurbit phloem exudates are largely from FP or are a mixture from both FP and EFP.

Rapid exudation from EFP presents methodological challenges for drawing correct conclusions regarding its true origin. This may be one reason why exudation sites were previously misinterpreted and assigned to FP (5, 6, 32). Unfortunately, most subsequent research on cucurbit phloem exudates and phloem transport has been based on these reports. Space precludes a full listing, but examples include (24, 33, 34, 35) and further examples are reviewed in (16, 21, 36). In light of the findings reported here, some conclusions may need to be carefully re-evaluated.

We have discovered huge divergence in metabolome and proteome contents between the two cucurbit phloem systems. This runs contrary to the notion that phloem represents a unified conduit. The new model of dual, functionally divergent transport systems provides a framework for future research using cucurbits as model species for studying phloem transport.

Phloem metabolite composition and transport. As mentioned in a recent review (19), since the very first extensive cucurbit phloem transport studies with radioactive tracers (37), it has been clear that stachyose and sucrose are the major forms of carbon exported from mature leaves. High rates of carbon mass flow in phloem are predicted from the fast growth of cucurbit vegetative and fruit tissues (25). However, no previous

reports showed high RFO content in cucurbit phloem exudates (for example: (15, 38). The total sugar content of around 1 M in FP is consistent with other species, and is in sharp contrast to the low sugar content of the extrafascicular exudate. The paradox of low sugar in the exudate is therefore now resolved. We can further conclude that sugar transport is, as always suspected, a major function of FP. Although internal FP was difficult to sample, there was no substantial difference between the composition of external and internal FP within the bicollateral stem vascular bundles, suggesting that they may have similar function. Extrafascicular phloem exudates contained abundant amino acids and many unidentified secondary metabolites (39), in contrast to the low levels of sugars. It is possible that some of these metabolites have protective functions, perhaps providing rings of defense both as the ectocyclic elements immediately below the epidermis and as the tissue surrounding each vascular bundle.

Phloem systems are divided into three functional zones: loading, transport and unloading (40). Cucurbit EFP systems are outside the photosynthate loading zone of leaf minor veins (41) and are therefore probably not involved in RFO loading. Further investigation is needed to assess whether EFP has roles in loading other molecules such as amino acids, or whether it has solely a transport function (42) that is responsible for collecting metabolites along transport systems of FP. The amino acid profile in exudates is similar to that from other species. This is consistent with a previous proposal that EFP may be specialized for delivering amino acids, based on immunolocalization of enzymes involved in nitrogen export (43).

Phloem protein composition. Consistent with the divergent metabolome composition between fascicular and extrafascicular phloem, gel analysis and LC/MS indicate that the proteomes are also substantially different. None of the dominant protein groups detected from FP feature as major components of EFP exudate. Conversely, the major exudate proteins PP1 and PP2 were not found in FP. The only evidence of shared proteins is based on close homology between the CmFPP1 peptides detected in this work and a protein present in the pumpkin phloem sap proteome (31). Further multiple homologous sequences in several species suggest that this protein is common to all cucurbits, and is a member of a small family (44). A more comprehensive comparative analysis of the proteomes from the two phloem systems will reveal how many proteins are common to

both systems. If the two systems have evolved from a single ancestral phloem, then retention of some sharing is likely.

Regarding protein function, we propose that PP1 and PP2 are responsible for the slow blocking of EFP that occurs over a period of several minutes after cutting, at which point the exudates become gel-like. However, we have shown that these proteins are, at most, only very low abundance components of FP. This is consistent with earlier observations (8, 9). However, FP is blocked almost instantaneously upon wounding, and this is unlikely to be due to PP1 and PP2. Although not yet tested experimentally, some of the major proteins detected from FP may have wound sealing functions.

In conclusion, we have shown that the two structurally and spatially distinct phloem systems in cucurbits have also evolved to be functionally differentiated and physiologically separated. This contrasts with the unified phloem systems present in most plant species. Evolution of functional divergence of phloem transport is not evident in other well-studied phloem model species, but may well exist outside the Cucurbitaceae. It remains to be seen whether the sum of the contents and functions in the two systems of cucurbits is equivalent to those in the single phloem of most other species. Although cucurbits cannot be considered a generic phloem model, they nevertheless represent models with unique advantages for phloem studies, because of their dual transport systems. The release of the complete cucumber genome sequence (30) will greatly facilitate such explorations.

Methods

Plant materials. Greenhouse-grown *Cucurbita maxima* Duch. cv. Gelber Zentner (pumpkin) was used for all studies, and compared to *Cucumis sativus* L. cv. Hoffmanns Giganta (cucumber) and *Cucurbita pepo* L. cv. Cocozelle v. Tripolis (zucchini) and *Citrullus lanatus* (Thunb.) Matsum. & Nakai (watermelon) for phloem exudation. Field-grown *Cucurbita maxima* cv. Atlantic Giant was used during later stages of phloem protein analysis. Three-month-old, mature plants (when stem phloem is fully developed) were used for metabolite analysis and for dissecting phloem proteins from fresh stem segments.

Microscopy. Full details are given in (Supporting Information: Text S1). Briefly, phloem exudation was observed by bright field and fluorescence stereo microscopy. Alkaline decolorized aniline blue was used as a callose stain, visualized under UV excitation. Carboxyfluorescein-5(6) [CF-5(6)] was used as a phloem-mobile tracer throughout, according to (27).

Sampling. Phloem exudates were collected according to (18) for metabolite and protein analysis. Fascicular phloem tissues for metabolite analysis were micro-dissected from freeze-dried stem segments of pumpkin. Fascicular phloem tissues for protein analysis were dissected from frozen pumpkin stem segments. Volumes of dissected tissues and percentage of sieve elements in dissected phloem tissues were estimated by microscopic measurement. Protein aggregates from FP sieve tubes were sampled directly with syringe needle tips from free-hand, fresh tissue sections of pumpkin stem after brief staining with 0.1% (w/v) amido black (pH ~ 6.8). Detailed protocols are given in Supporting Information (Text S1).

Metabolite and protein analysis. Metabolite profiling and identification from phloem exudates and dissected tissues were done according to (18, 29, 39). Proteins collected from FP by needle tips were processed either by direct acetone precipitation or phenol method (45). Proteins from dissected FP tissues were extracted by phenol method. Extracted proteins were analyzed by 1D or 2D-SDS-PAGE. Protein extracts of needle-dissected protein aggregates and from excised gel bands or spots were also analyzed, after trypsin digestion, by nano LC/MS/MS. MASCOT database searching was performed according to standard procedures. *De novo* sequencing was conducted with methods reported by (34). Full details of analytical methods are given in Supporting Information: Text S1*)*.

Acknowledgements Financial support from Max Planck Society (2000-2003) to BZ, VT, OF and from DDPSC to BZ and LMH are acknowledged. Many thanks to Dr. Julia Kehr for initial sequencing of tryptic peptides, Greg Dulski for providing *Cucurbita maxima* cv. Atlantic Giant plant materials, Bert Berla and Dr. Sophie Alvarez for assistance with 2D-SDS-PAGE, and Prof. Robert Turgeon for constructive comments on an earlier version of the manuscript. There are no competing interests.

Reference

1. Fisher DB (2002) Long-distance transport. *Biochemistry & Molecular Biology of Plants*, ed Clarke AE (John Wiley & Sons).
2. Ruiz-Medrano R, Xoconostle-Cazares B, Lucas WJ (2001) The phloem as a conduit for inter-organ communication. *Curr Opin Plant Biol* 4(3):202-209.
3. van Bel AJE (2003) The phloem, a miracle of ingenuity. *Plant, Cell & Environment* 26(1):125-149.
4. Fisher A (1883) Das Sieboehren system von Cucurbita. The phloem system of *Cucurbita* (German) *Ber deutsch botGes* 1:276-279
5. Crafts AS (1932) Phloem anatomy, exudation and transport of organic nutrients in cucurbits. *Plant Physiol* 7:183--225.
6. Crafts AS (1936) Further studies on exudation in cucurbits. *Plant Physiol* 11:63--79.
7. Eschrich W, Evert RF, Heyser W (1971) proteins of the sieve tube exudate of *Cucurbita maxima*. *Planta* 100:208-221.
8. Smith LM, Sabnis DD, Johnson RPC (1987) Immunocytochemical localization of phloem lectin from *Cucurbita maxima* using peroxidase and colloidal-gold labels. *Planta* 170(4):461-470.
9. Clark AM, *et al.* (1997) Molecular characterization of a phloem-specific gene encoding the filament protein, phloem protein 1 (PP1), from *Cucurbita maxima*. *Plant J* 12(1):49-61.
10. Kempers R, Prior DAM, van Bel AJE, Oparka KJ (1993) Plasmodesmata between sieve element and companion cell of extrafascicular stem phloem of *Cucurbita maxima* permit passage of 3-Kda fluorescent-probes. *Plant J* 4(3):567-575.
11. Lalonde S, Tegeder M, Throne-Holst M, Frommer WB, Patrick JW (2003) Phloem loading and unloading of sugars and amino acids. *Plant Cell Environ* 26(1):37-56.
12. Turgeon R, Medville R (1998) The absence of phloem loading in willow leaves. *PNAS* 95(20):12055-12060.
13. Turgeon R (1996) Phloem loading and plasmodesmata. *Trends Plant Sci* 1(12):418-423.
14. Schaffer AA, Pharr DM, & Madore MA (1996) Cucurbits. *Photoassimilate Distribution in Plants and Crops : Source-sink Relationships*, ed Schaffer AA (Marcel Dekker, New York), pp 729--753.
15. Richardson PT, Baker DA, Ho LC (1982) The chemical composition of cucurbit vascular exudates. *J Exp Bot* 33(137):1239-1247.
16. Thompson GA (1999) P-Protein trafficking through plasmodesmata. *Plasmodesmata: Structure, Function, Role in Cell Communication*, ed van Bel AJE, van Kesteren WJP (Springer Verlag), pp 295-314.
17. Haritatos E, Keller F, Turgeon R (1996) Raffinose oligosaccharide concentrations measured in individual cell and tissue types in *Cucumis melo* L leaves: Implications for phloem loading. *Planta* 198(4):614-622.
18. Fiehn O (2003) Metabolic networks of *Cucurbita maxima* phloem. *Phytochemistry* 62(6):875-886.
19. Turgeon R, Wolf S (2009) Phloem transport: cellular pathways and molecular trafficking. *Annu Rev Plant Biol* 60(1):207-211
20. Oparka KJ, Cruz SS (2000) The great escape: Phloem transport and unloading of macromolecules. *Annu Rev Plant Phys* 51:323-347.
21. Thompson GA, Schulz A (1999) Macromolecular trafficking in the phloem. *Trends Plant Sci* 4(9):354-360.
22. Evert RF, Eschrich, Eichhorn SE (1973) P-protein distribution in mature sieve elements of *Cucurbita maxima*. *Planta* 109(3):193-210.
23. Petersen MIC, Hejgaard J, Thompson GA, Schulz A (2005) Cucurbit phloem serpins are graft-transmissible and appear to be resistant to turnover in the sieve element-companion cell complex. *J Exp Bot* 56(422):3111-3120.
24. Golecki B, Schulz A, Thompson GA (1999) Translocation of structural P proteins in the phloem. *Plant Cell* 11(1):127-140.
25. Crafts AS, Crisp CE (1971) *Phloem transport in plants* (W.H. Freeman, San Francisco,).
26. Esau K (1965) *Plant anatomy* (Wiley, New York,) 2d Ed.

27. Grignon N, Touraine B, Durand M (1989) 6(5)Carboxyfluorescein as a tracer of phloem sap translocation. *Am J Bot* 76(6):871-877.
28. Knoblauch M, van Bel AJE (1998) Sieve tubes in action. *Plant Cell* 10(1):35-50.
29. Tolstikov VV, Fiehn O (2002) Analysis of highly polar compounds of plant origin: Combination of hydrophilic interaction chromatography and electrospray ion trap mass spectrometry. *Anal Biochem* 301(2):298-307.
30. Huang S, *et al.* (2009) The genome of the cucumber, *Cucumis sativus* L. *Nature genetics* 41(12):1275-1281.
31. Lin MK, Lee YJ, Lough TJ, Phinney BS, Lucas WJ (2009) Analysis of the pumpkin phloem proteome provides insights into angiosperm sieve tube function. *Mol Cell Proteomics* 8(2):343-356.
32. Eschrich W, Evert RF, Heyser W (1971) Proteins of sieve-Tube exudate of *Cucurbita maxima*. *Planta* 100(3):208-221.
33. Yoo BC, Lee JY, Lucas WJ (2002) Analysis of the complexity of protein kinases within the phloem sieve tube system. Characterization of *Cucurbita maxima* calmodulin-like domain protein kinase 1. *J Biol Chem* 277(18):15325-15332.
34. Walz C, Juenger M, Schad M, Kehr J (2002) Evidence for the presence and activity of a complete antioxidant defence system in mature sieve tubes. *Plant J* 31(2):189-197.
35. Xoconostle-Cazares B, *et al.* (1999) Plant paralog to viral movement protein that potentiates transport of mRNA into the phloem. *Science* 283(5398):94-98.
36. Lough TJ, Lucas WJ (2006) Integrative plant biology: role of phloem long-distance macromolecular trafficking. *Annu Rev Plant Biol* 57:203-232.
37. Webb JA, Gorham PR (1964) Translocation of photosynthetically assimilated C14 in straight-necked squash. *Plant Physiol* 39(4):663-672.
38. Mitchell DE, Gadus MV, Madore MA (1992) Patterns of assimilate production and translocation in muskmelon *Cucumis Melo* L. I. diurnal patterns. *Plant Physiol* 99 (3):959-965.
39. Tolstikov VV, Fiehn O, Tanaka N (2007) Application of Liquid Chromatography-Mass Spectrometry Analysis in Metabolomics. *Metabolomics: Methods and Protocols,* Methods in Molecular Biology (Vol.358), (The Humana Press Inc., Totowa, NJ, USA), pp 141-155.
40. van Bel AJE (1993) The transport phloem: specifies of its functioning. *Progress in Botany*, (Springer), Vol 54, pp 134-150.
41. Turgeon R, Webb JA, Evert RF (1975) Ultrastructure of minor veins in *Cucurbita pepo* leaves. *Protoplasma* 83(3):217-232.
42. van Bel AJE (1993) The transport phloem: specifies of its functioning. *Progress in Botany* 54:134-150.
43. Chen ZH, *et al.* (2000) Are isocitrate lyase and phosphoenolpyruvate carboxykinase involved in gluconeogenesis during senescence of barley leaves and cucumber cotyledons? *Plant Cell Physiol* 41(8):960-967.
44. Omid A, Keilin T, Glass A, Leshkowitz D, Wolf S (2007) Characterization of phloem-sap transcription profile in melon plants. *J Exp Bot* 58(13):3645-3656.
45. Hurkman WJ, Tanaka CK (1986) Solubilization of Plant Membrane Proteins for Analysis by Two-Dimensional Gel Electrophoresis *Plant Physiol* 81:802-806.

Figure Legends

Table 1. RFO sugar concentrations in different tissues measured by LC/MS.
The first two rows show the RFO sugar concentration, which was calculated based on the total volume of dissected external and internal fascicular phloem tissues. The third and fourth rows show the estimated RFO sugar concentration in external and internal fascicular SE/CCCs. The last three rows show RFO sugar concentrations calculated

from total sample volume. Number format: Mean ± Standard error. Unit of concentration: mM; N: number of observations. N.D.: not detected.

Fig. 1. Direct observation of phloem exudation from stem of *Cucurbita maxima* (pumpkin). ***A*:** Initial spreading of rapidly exuding sap over the entire cut stem surface. Bicollateral vascular bundles containing both internal and external fascicular phloem (IP, EP in B.) were readily identified by their dark green color and the distinctive intervening xylem region (X). Arrowheads: glistening exudates under illuminating light; ***B*:** Close-up of boxed region in A; ***C*-*H*:** Approx 30 s later, after removal of sap with filter paper, exudation has slowed. Images shown are selected frames from video record of subsequent slower exudation. The full video is available at Supporting Information: Video S1. Times are from the last removal of exudate with filter paper. Droplets of exudate (red arrowheads) can clearly be seen from extrafascicular phloem sites surrounding fascicular phloem region, and from extrafascicular phloem regions in cortex. In no case was exudation seen to originate from fascicular phloem. Image brightness and contrast have been modified for enhanced clarity. ***I***: UV fluorescence image of part of the vascular structure after DAB staining. Arrowhead: one droplet of exudate was still formed from extrafascicular phloem, even after staining. CO: cortex.

Fig. 2. Examination of sites of pumpkin phloem exudation by phloem-mobile fluorescent tracer. Epifluorescence stereomicroscope images of cut surfaces following application of CF5(6) phloem-mobile tracer to distant tissues. ***A, B*:** petiole cut surface after applying CF5(6) to intact leaf surface; ***C*:** stem cut surface, after applying CF5(6) to intact leaf surface. ***D* – *F*:** petiole cut surface after applying CF5(6) to distal intact petiole surface. Only part of the surface is shown, including one or a few vascular bundles.

A: Spreading of fluorescent exudates over petiole surface immediately after cutting. Fascicular phloem regions were intensely labeled. Arrow points to a discrete phloem exudate droplet from extrafascicular phloem region outside internal fascicular phloem. ***B***: Exudation from cut petiole eventually stops after repeated removal of exudates. Both fascicular phloem and extrafascicular phloem remain labeled, including commissural sieve tubes (CS), which belong to extrafascicular phloem. Arrows indicates small bright

dots in extrafascicular phloem. ***C***: Stem surface immediately after cutting shows labeled fascicular phloem. Arrow indicates faint spreading of label from external fascicular phloem, interpreted as being derived from broken sieve tubes. ***D***: Labeled phloem exudates spread on petiole cut surface. White arrows point to smaller exudate droplets from cortical extrafascicular phloem elements not adjacent to vascular bundles. Red arrow points to vascular bundle region. Neither external nor internal fascicular phloem was labeled. Inset picture shows background autofluorescence of control petiole without CF5(6). ***E***: After repeated removal of exudates from cut petiole surface, droplets continued to form and were still labeled. Fascicular phloem (EP and IP) appear as more yellow-green indistinct regions. These regions are unlabeled or minimally labeled (compare with *A – C*) and do not underlie the exudate droplets. ***F***: Petiole surface shown in *E* was counter-stained with DAB and then re-photographed. Light blue specks indicate sieve elements and delineate both fascicular phloem regions. Exudate droplets are from extrafascicular phloem near to fascicular phloem, but not from fascicular phloem itself.

X: xylem; EP: external fascicular phloem; CS: commissural sieve tubes, IP: internal fascicular phloem. Scale bar in A, B, E, F = 400 µm, in C = 2 mm, in D = 1 mm.

Fig. 3. Metabolite profiles of dissected fascicular phloem tissues and phloem exudates. ***A – C***: GC/MS profiles. ***A***: Total ion chromatogram (TIC) of phloem exudates. ***B***: TIC of dissected external fascicular phloem tissues. ***C***: overlay of extracted ion chromatograms from *B,* to emphasize the major components detected in fascicular phloem tissues. cps: unit of absolute GC/MS signal intensity in counts per second. ***D – F***: LC/MS profiles. ***D***: TIC of phloem exudates. ***E***: TIC of dissected external fascicular phloem tissues. ***F***: average of full scan mass spectra for marked chromatogram segment in bracketed region in *D,* indicating the glycan series present in phloem exudates but not in fascicular phloem. Panel ***F*** displays the $(M+H)^+$ ions of all major glycans detected in phloem exudates, with the 162 m/z increment (one hexose unit) starting from either of the two aglycones (268.2 and 296.2 m/z, respectively).

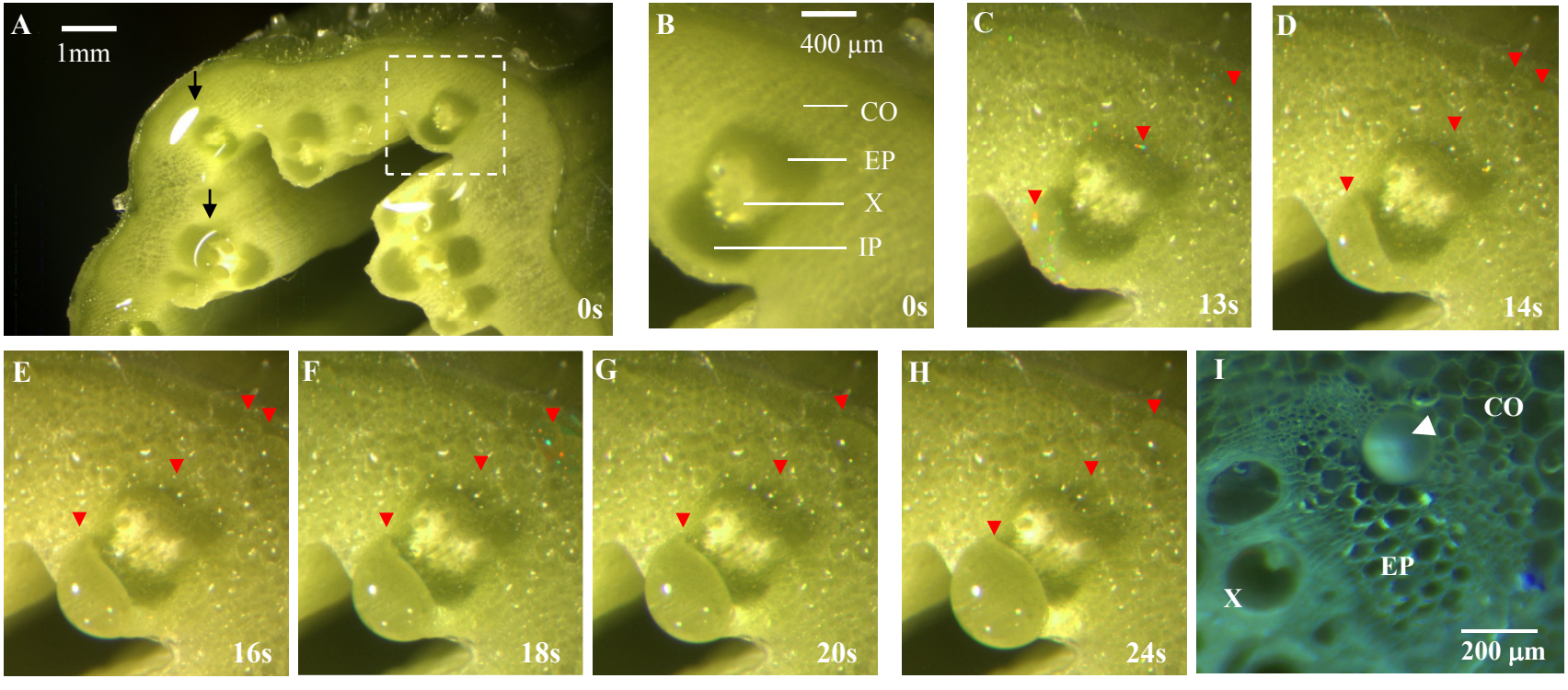
Fig. 4. Comparing proteome contents between pumpkin phloem exudates and fascicular phloem. ***L***: SDS-PAGE (10%): Lanes A-E represent: phloem exudates,

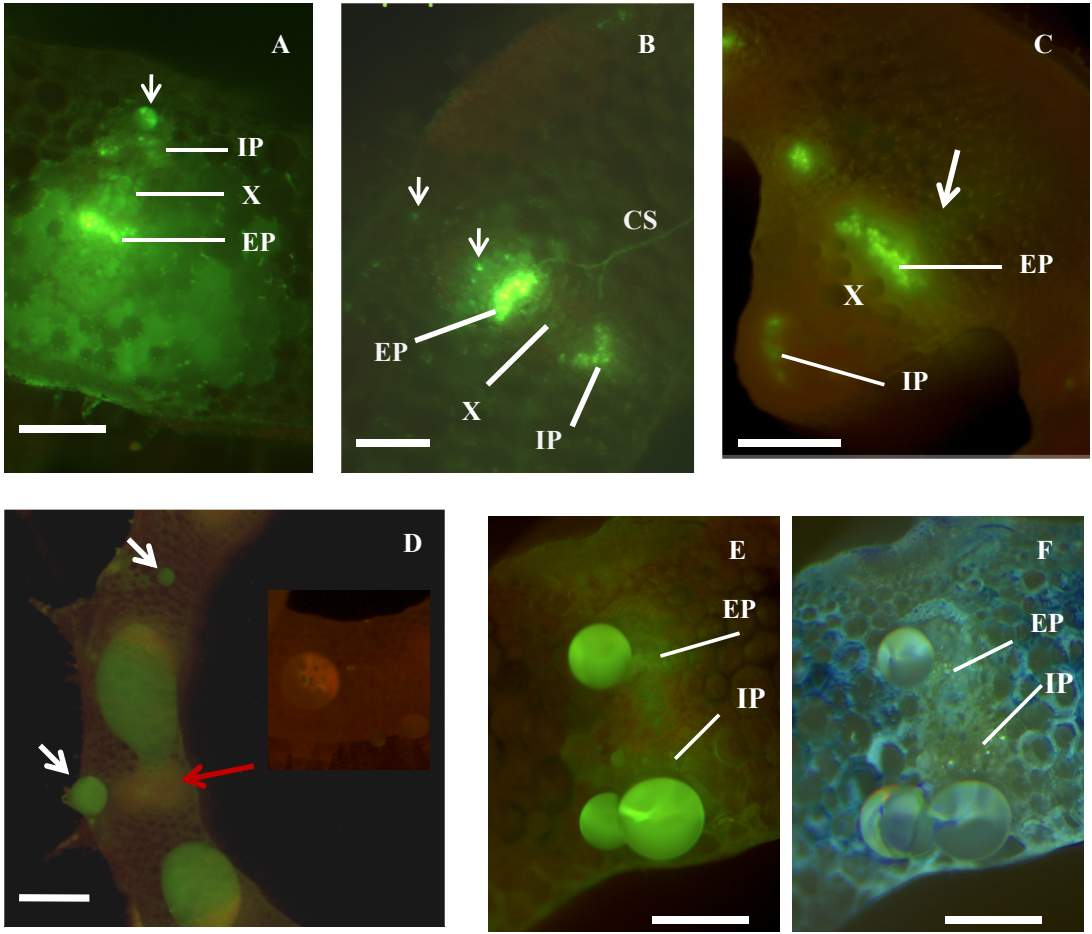
523 dissected external fascicular phloem extracts, dissected internal fascicular phloem
524 extracts, molecular weight markers and fascicular phloem proteins sampled by needle
525 tips, respectively. MW markers: from top to bottom, 200, 150, 100, 75, 50, 37, 25, 20,
526 kDa. PP1 and PP2 are the most abundant proteins in pumpkin phloem exudates. ***R***: 2D-
527 PAGE of fascicular phloem proteins sampled by needle tips. IEF: pI 3-10 non-linear;
528 SDS-PAGE: 8%-16%. MW markers: 200, 150, 100, 75, 50, 37, 25, 20, 15, 10 kDa. For
529 both gels, arrows indicate one of the major fascicular phloem proteins, designated as
530 CmFPP1, which is a single band in 1D gel (left) and two longitudinal smeared bands in
531 2D gel (right).

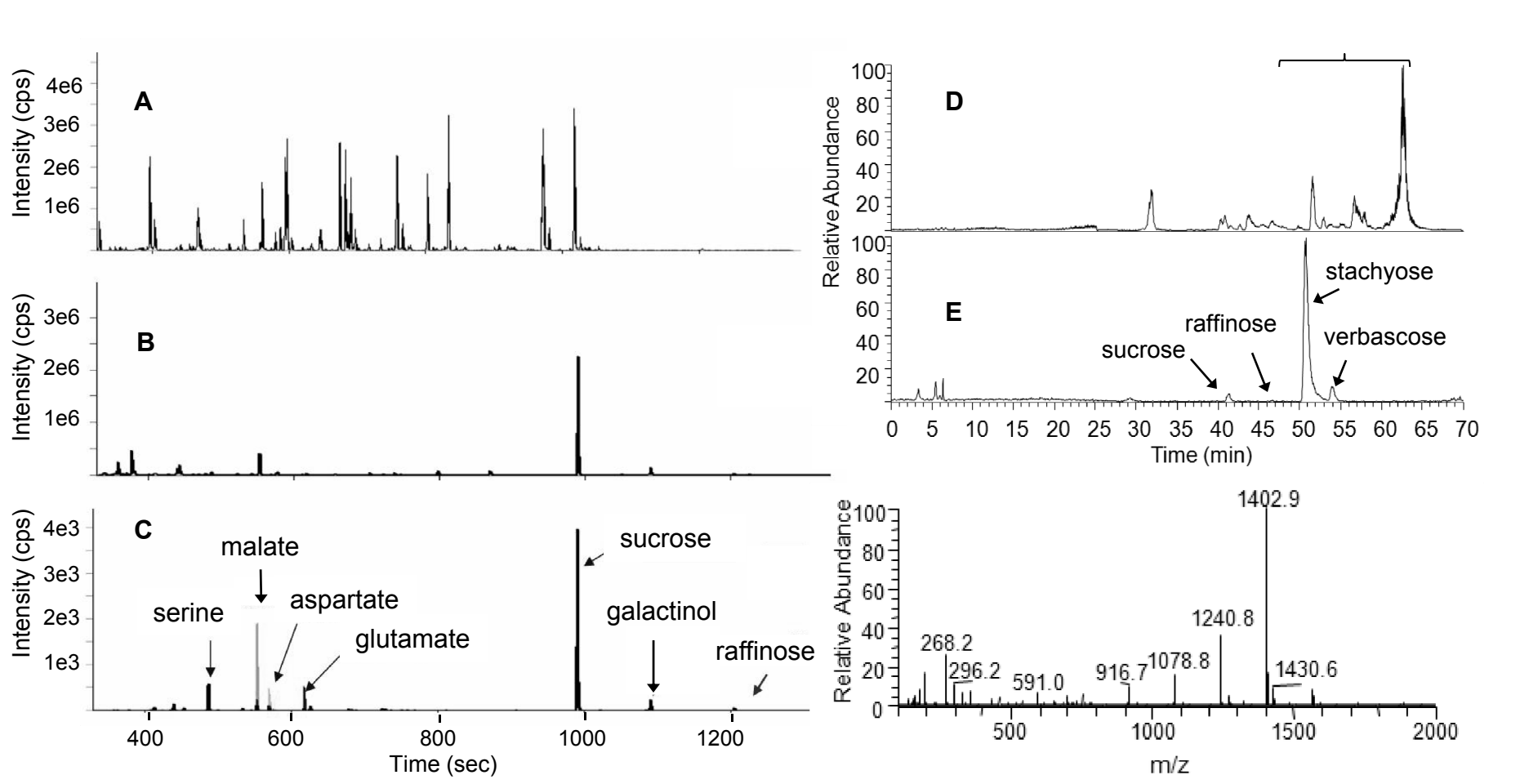
532

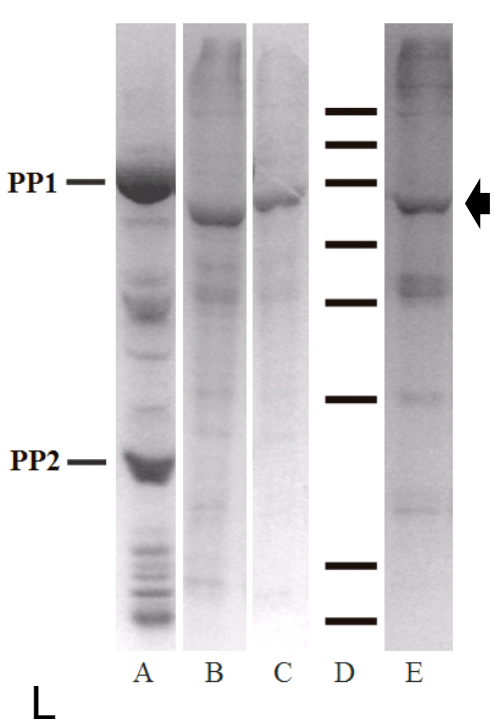
533

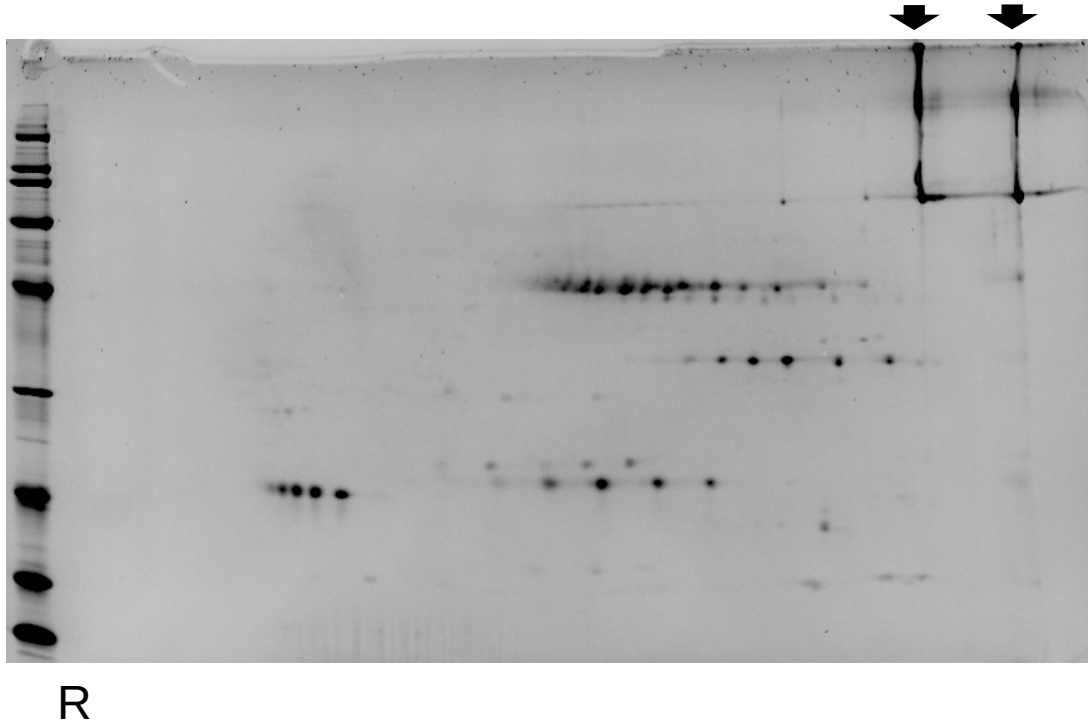
Tissue Type	Sucrose	Raffinose	Stachyose	Verbascose	Sum of RFOs	N
Total dissected external fascicular phloem tissue	60.0 ± 9.8	14.0 ± 2.4	521.0 ± 126.1	55.9 ± 14.5	651.0 ± 142.4	12
Total dissected internal fascicular phloem tissue	43.2 ± 27.1	N.D	425.9 ± 269.7	79.7 ± 51.4	548.7 ± 348.3	2
External fascicular phloem SE/CCC (by estimation)	88.3 ± 17.5	6.6 ± 4.3	908.0 ± 224.1	81.1 ± 25.7	1139.1 ± 253.2	12
Internal fascicular phloem SE/CCC (by estimation)	58.4 ± 48.3	N.D.	738.7 ± 479.5	123.3 ± 91.4	957.2 ± 619.2	2
Leaf disc	3.1 ± 0.7	3.8 ± 0.6	9.0 ± 1.5	0.5 ± 0.1	16.5 ± 2.3	6
Phloem exudate	0.4±0.6	17.5±18.8	9.5±12.1	1.7±2.9	29.4±34.3	3
Xylem	0.7 ± 0.3	0.1 ± 0.0	5.2 ± 2.6	1.5 ± 0.9	7.4 ± 2.8	4


A
1mm
0s
B
400 µm
CO
EP
X
IP
0s
C
13s
D
14s
E
16s
F
18s
G
20s
H
24s
I
CO
EP
X
200 µm


A
IP
X
EP
B
CS
EP
X
IP
C
EP
X
IP
D
E
EP
IP
F
EP
IP


A
B
C
D
E
Intensity (cps)
4e6
3e6
2e6
1e6
3e6
2e6
1e6
4e3
3e3
2e3
1e3
malate
serine
aspartate
glutamate
sucrose
galactinol
raffinose
400
600
800
1000
1200
Time (sec)
Relative Abundance
100
80
60
40
20
stachyose
raffinose
sucrose
verbascose
0
5
10
15
20
25
30
35
40
45
50
55
60
65
70
Time (min)
1402.9
1240.8
268.2
296.2
591.0
916.7
1078.8
1430.6
500
1000
1500
2000
m/z


PP1
PP2
A
B
C
D
E
L


R

Supporting Information:

Video S1: Video record of phloem exudation process in pumpkin

The video also available online at http://www.danforthcenter.org/cmaxima/. Selected still images from this video are shown in Fig. 1.

Fig S1: Scheme of phloem tracer experiments and summary of all experimental evidence for testing origins of phloem exudation in cucurbits.

Scheme shows the three different types of observations in CF5(6) tracer experiments for discerning the origin of phloem exudates. Below is a summarized list of all experimental evidence based on working scheme above (Expt: abbreviation for experiment):

Expt 1: Direct observation of exudation

Observations: Exudates originated from positions of EFP, not FP
Conclusions: Exudates may not from FP, but from EFP.

Expt 2a: Feed CF5(6) to leaf blade

Observations: Both phloems in petioles are labeled (Fig 2A, 2B)
Conclusions: CF5(6) is phloem limited, both phloems are effective in CF transport, but cannot use this to distinguish source of exudates.

Expt 2b: Feed CF5(6) to leaf blade

Observations: Only FP is labeled in distant stem: not exudates, not EFP (Fig 2***C***)
Conclusions: Exudates is from EFP.

Expt 3: Feed CF5(6) to petiole surface (transport phloem)

Observations: Petiole FP is not labeled but exudates is (Fig 2***D***,2***E***,2***F***)
Conclusions: exudate is not from FP.

Fig S2: Dissected pumpkin fascicular phloem tissues used for metabolite analysis.

An example procedure to dissect lyophilized central phloem tissue from vascular bundles. ***A*** Lyophilized stem segments were dissected under stereo microscope with sharp razor blades. ***B*** Dissected fascicular phloem tissues. ***C*** Purity was confirmed with decolorized aniline blue staining of both ends of dissected tissues. Stained callose deposits indicate sieve plates and pore-plasmodesmal units. EFP: exterfascicular phloem; FP: fascicular phloem.

Fig S3: Sampling fascicular phloem proteins by needle tips.

A: Longitudinal free-hand sections of living stem vascular bundles, stained with amido black 10R for proteins. Red arrow indicates stained proteins in extrafascicular phloem; Yellow arrows indicate protein strands from fascicular phloem, which were collected on needle tips. ***B***: Stem cross sections; for abbreviations see Fig S2. Yellow arrow indicates FP proteins stretched by needle-tip. ***C***: Needle tip with attached amido-black-stained fascicular phloem proteins (dark blue). ***D***: Sampled stained proteins under light microscope. ***E***: Sampled proteins under epifluorescent microscope. Yellow arrow: sieve plates with callose staining.

Fig S4: 2D-PAGE of phloem exudates and phospho-stained fascicular phloem proteins on 2D-gel from *Cucurbita maxima*.

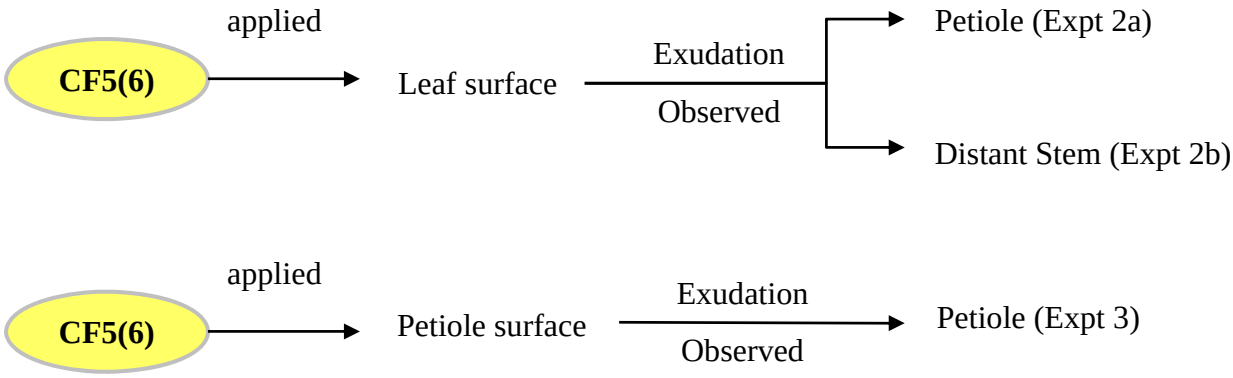
A: Under standard 2D-PAGE electrophoresis conditions, the abundant PP1 and PP2 proteins appear as horizontal smear lines along IEF dimension (as indicated). However, smearing does not affect the identification of these proteins. Analysis conditions for proteins from phloem exudates were identical to those used for dissected fascicular phloem proteins shown in Fig. 4. ***B***: Subsequent phospho-protein staining of the same gel (in Fig A) by Pro-Q Diamond to visualize possible phosphorylated proteins in exudated protein extracts. No phosphorylated proteins from phloem exudates were detected. ***C***: 2D-PAGE of fascicular phloem proteins visualized by Sypro-staining. CmFPP1 appears as horizontal smear lines along IEF dimension (as indicated). ***D***: Subsequent phospho-protein staining by Pro-Q Diamond revealed one group of phosphorylated proteins from fascicular phloem (as indicated). IEF: pI 3-10 non-linear; SDS-PAGE: 8%-16%. MW markers: 200, 116, 97, 66, 45, 31, 21, 14, 6 kDa.

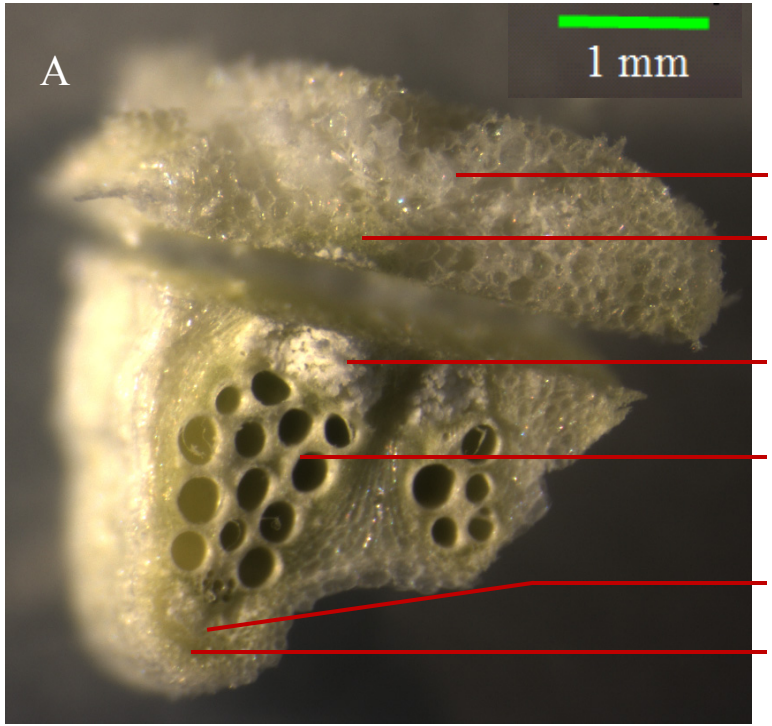
Table S1: CLUSTAL alignment of partial sequences from cucumber genome and pumpkin proteome with peptides identified from CmFPP1.

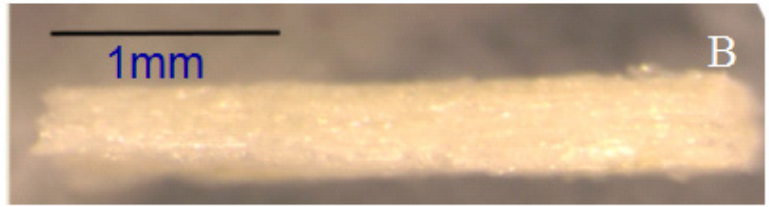
Cs_contigxxxxx cucumber sequences are from NCBI Genome Project ID 33619 by The Cucumber Genome Initiative (1) FGxxxxx_x sequences are from pumpkin sap proteome accessions with xxkD suffix indicating predicted molecular weight (2).Sequences in underlined red are peptides identified from CmFPP1 matched onto closest homologous sequence, FG227702_3_81kD. Shorter homologous sequences were also found from watermelon and melon (Accessions WMN55A06 and MU9468, respectively, at www.icugi.org).

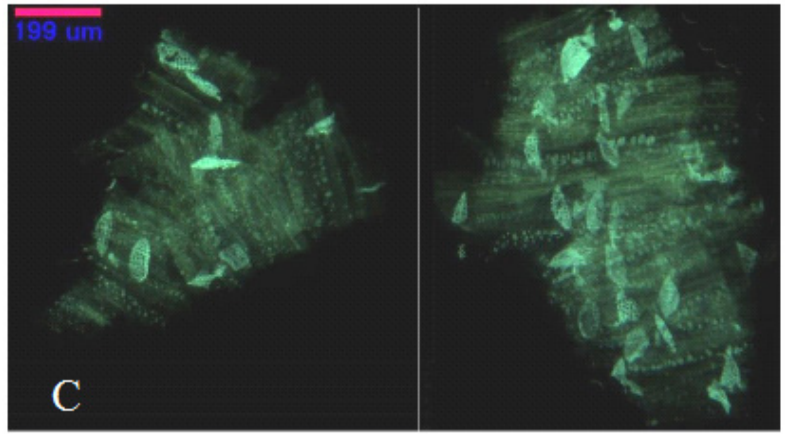
References

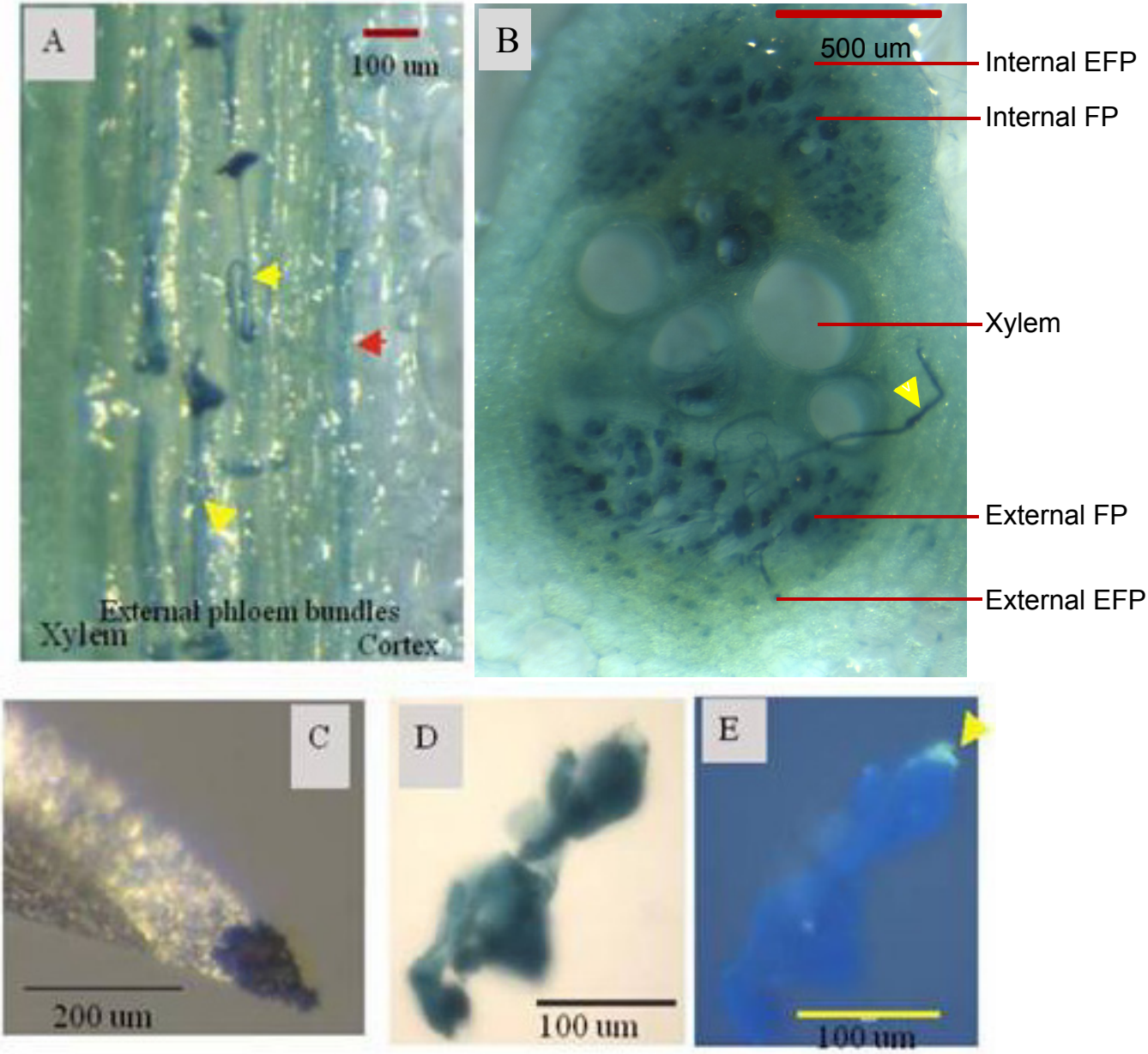
1. Huang S, *et al.* (2009) The genome of the cucumber, Cucumis sativus L. *Nature genetics* 41(12):1275-1281.
2. Lin MK, Lee YJ, Lough TJ, Phinney BS, Lucas WJ (2009) Analysis of the pumpkin phloem proteome provides insights into angiosperm sieve tube function. *Mol Cell Proteomics* 8(2):343-356.

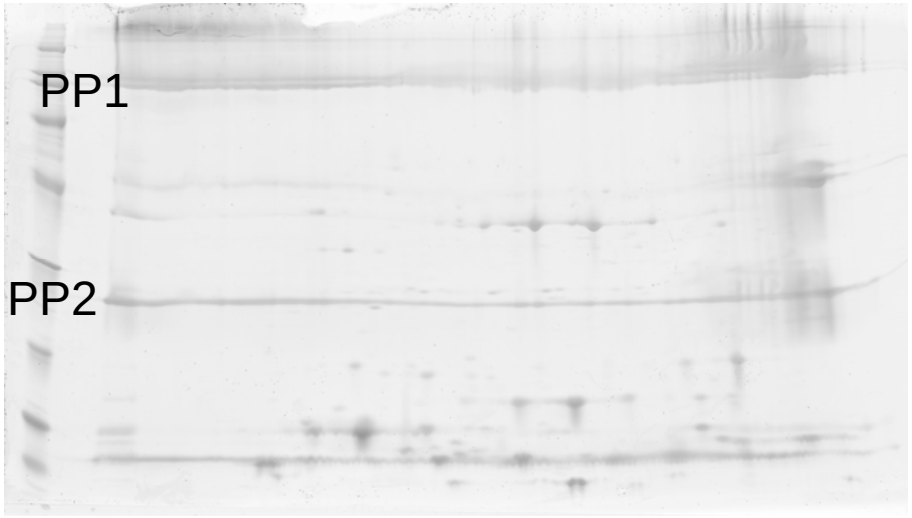

applied
CF5(6)
Leaf surface
Exudation
Observed
Petiole (Expt 2a)
Distant Stem (Expt 2b)
applied
CF5(6)
Petiole surface
Exudation
Observed
Petiole (Expt 3)


A
1 mm
Cortex
External
EFP region
External FP
Xylem
Internal FP
Internal
EFP region

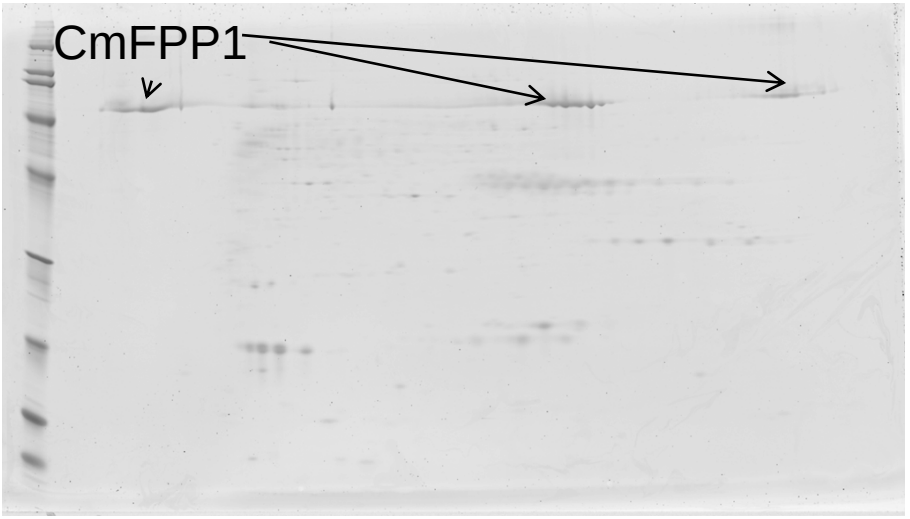

1mm
B


199 um
C


A
100 um
External phloem bundles
Xylem
Cortex
B
500 um
Internal EFP
Internal FP
Xylem
External FP
External EFP
C
200 um
D
100 um
E
100 um



A: Phloem exudates proteins (Sypro-stained)



C: Central phloem proteins (Sypro-Stained)



B: Phloem exudates (Pro-Q Diamond Phosphoprotein stained after sypro-staining in A)



D: Central phloem proteins (Pro-Q Diamond Phosphoprotein stained after sypro-staining in C)

```
FG227020 2 56kD      YCTDELK-REDNYKIVWIPMINSQGFDQE--SR 106
Cs contig13022          EELK-REDNYKIVWIPVMNSEAFNEE--SH 27
Cs contig12984          NEVK-REDKYKIVWIPVITVETEDEEEEAR 29
Cs contig12982          DELG-REDKYKIVWIPIINPNEPYEE--NR 27
Cs contig13025       HVYNELK-RDNKYEIVWIPIIPERYLEED---R 29
FG227702 3 81kD      NVYDELKNRGTNYEIVWIPIIPEPYHEDD---H 357
Cs contig13028          EELK-RDNRYEIVWIPIIPEPYQEED---R 26
                         *:  *   * *****::       :

FG227020 2 56kD      KRYELVRSTMKWYAVQYTTKIAGLRFLEEIWQVREDALMVVLDSKSKVKFSNAIHLLRVW 166
Cs contig13022       KRYENLRSTMKWYAVQYGTKIAGLRFLEEIWQLRDDALMVVLDSKSKLKFSNAIHLLRVW 87
Cs contig12984       KKYEYASSLMKWYIVPYTRKIAGWRYLEENWQLRQDPLIVVMNSKSRVEFNNAIHLIRVW 89
Cs contig12982       RRYEYVISKMPWYIVQFTTKIAGWRFLEENWQLRDDPLVVVLDSTSKVEFTNAIHLIRVW 87
FG227362 3 45kD      ---EYLRSTMKWYSMQFTTRVAGMRYIEEKWQLREDPLVVVLNPQSKVEFTNAIHLIRVW 57
Cs contig13025       RRYEYLRSTMKWYSIQFTTRIAGMRYIEEKWQFREDPLVVVLNPQSKVEFTNAIHLIRVW 89
FG227702 3 81kD      KKYEYLRSTMKWYSIQFTTKISGMRYLEEKWQLREDPLVVVLSPQSEVVFMNAIHLIRVW 417
Cs contig13028       KRYEYLRSTMKWYSVEFTTKISGMRYIEEKWQLREDPLVVVLNPQSKVEFMNAIHLIRVW 86
                     ::**   * * ** : :  :::* *::** **.*:*.*:**:.. *.: * *****:***

FG227020 2 56kD      GNNAIPFTVERANALLRKNWPESTIVKFINQPRLQSWID--------------------Q 206
Cs contig13022       GNNAIPFTLERANALLRKNWPESTIVKFTNQPRLQSWIID------------------Q 128
Cs contig12984       GIDAIPFTNGRTNALLAKNWPESTLFKFIDQPRLMNWVSHV-----------------NQ 132
Cs contig12982       GSEVVPFSNRKIDILLEKTWPESTILKFTDHPRVHNWVSK-----------------NQ 129
FG227362 3 45kD      GTEAIPFTHNRTEILLRKHWPESTLVKFTHQPRLLSW--------------------FNQ 97
Cs contig13025       GTEAIPFTHNRTDYLLRKHWPESTLVKFTHQPRLLSWVRILFNMTRAPLFDNHFVLGFNQ 149
FG227702 3 81kD      GTEAIDFKEDRAKFLLRKNWPDSTLVKFTHQPRLQSWIK--------------------Q 457
Cs contig13028       ENEAFPFTLDRTQALLRRNWPESTLIKFTHQPRLQNWVLSK---------------QIAR 131
                       :.. *.  : . ** : **:**:.** .:**: .*                     :

FG227020 2 56kD      GRSIIFYGGKDQDWIQGFEEKVVDIKNDRSMRESGINFEIVRIGNNN-----DNNNASFM 261
Cs contig13022       EKTIIFYGGKDIDWIQKFEEKVVDIKNDRSMRDNGITFEIVHIGINKNTTKGEDDNNSNM 188
Cs contig12984       ERNIIFYGGKEPKWIQQFEDRIVEIKNDPYLKEKGNTFEIIRVGQNIK---GDSNDFTLT 189
Cs contig12982       EKNIIFYGGKDPNWIQQFEEKVIDIKTDPWIRSKGITFEIVRIIRDD--------DPKLM 181
FG227362 3 45kD      ERSILFYGGKEPKWIQQFEERAEFLKSDPLVIE-GRSFEIVRIGKNAR----GEDDPALM 152
Cs contig13025       EKSILFYGGKDPKWIQQFEERTEILKSDPLIIE-GRSFEIVRIGKNAR----GEEDPALM 204
FG227702 3 81kD      EKSILFYGGKEPMWIQQFEERVEILKSDPLIRD-GGSFEIVRIGKNAK----GEDDPALM 512
Cs contig13028       DKNILFYGGKDPLWIQQFEERAEILRSDPLIMD-GGSFEIVRIGKDAI----GQDDPALM 186
                      :.*:*****:  *** **::   ::.*  : . * .***:::  :         :

FG227020 2 56kD      SRFWITQWGFFVVKSQLTGSSASETTEDILRLISYENENGWAILTVGSAPLLVGRGNLIL 321
Cs contig13022       ARFWISQWGFFIIKSQLTGSSASETTEDILRLISYENENGWAILTVGSAPLVVARGNLVL 248
Cs contig12984       PQFWLTQWGYFVIKSQLKGSSATETTEDILRLISYENENGWAIVAVGSTPLLVGRGNLIM 249
Cs contig12982       SRFWITQWGFFIVKSQIKGSSASETTEDILRLISYENENGWGILAVGSEPVLVGRGNLIL 241
FG227362 3 45kD      ARFWKTQWGYFIIKSQIKGSNASETTEDILRLISYENEDGWAVLTVGPTPILVGRGLLIL 212
Cs contig13025       ARFWTTQWAYFIIKSQLKGSSASETTEDILRLISYENENGWVVLTVGPAPLLVGRGFLIL 264
FG227702_3_81kD      ARFWKIQWGYFIVKSQLIGSSASETTEDILRLISYQNEEGWVVLSVGSAPVLVGRGILIL 572
Cs contig13028       ARFWTTQWGYFVVKSQIKGSSASETTEDILRLISYQNEDGWVVLTVGTAPVLVGRGILIL 246
                     .:**  **.:*::***: **.*:************:**:** :::**. *::*.** *::

FG227020 2 56kD      RVFEDFNRWKKNLNLKGFPNAFQDYFNEMALETHQCERVTLPGFSGWIPMIVNCPECPRF 381
Cs contig13022       GVFEDLNAWKKNLNLKGFPNSFKDYFEQLALRTHQCEKVILPGFSGWIPMIVNCPECPRF 308
Cs contig12984       GVLQDFNKWKRNMNIKAFPDAFRDYFNELNLNFHICERMTLPGFSGWIPMIVNCPECPRF 309
Cs contig12982       AVLQDFNKWKQILNIKSFPDSFRDYFNELALKTHQCDRVVLPGFSGWIPMVVNCPECPRF 301
FG227362 3 45kD      RLLEDFPKWKQMLRLKGFPDAFRENFNELAAKTHQCDRVILPGFSGWIPMIVNCPECPRF 272
Cs contig13025       RLLEDFPKWKQTLRLKGFPDAFREYFNELAAKNHQCDRVILPGFSGWIPMIVNCPECPRF 324
FG227702_3_81kD      KLLEEFPKWKQSLRLKAFPDAFREYFNELALKSHQCDRVILPGFSGWIPMIVNCPECPRF 632
Cs contig13028       KLLEDFPKWKQNLRIKAFPDVFREYFNELAFSSHQCDRVILPGFSGWIPMIVNCPECPRF 306
                      :::::  **: :.:*.**: *:: *:::    * *::: **********:*********

FG227020 2 56kD      METGINFNCCHGR 394
Cs contig13022       METGINFNCCHGR 321
Cs contig12984       METGISFKCNHGR 322
Cs contig12982       MDTGISFKCCHGR 314
FG227362 3 45kD      METGISFKCCHGR 285
Cs contig13025       METGISFKCCHG- 336
FG227702_3_81kD      METGISFKCCHGG 645
Cs contig13028       METGISFKCCHG- 318
                     *:***.*:* **
```

Supplementary Methods

Microscopic observation. Phloem exudation was observed by bright field and fluorescence stereo microscopy (MZFLIII, Leica, Germany). To increase working distance below objectives, the microscope head was mounted on a metal stand, below which potted plants were placed. To allow immediate observation, focus was pre-adjusted before the stem or petiole was cut transversely with a clean scalpel. There was no noticeable difference in exudation pattern from upper and lower faces of the cut stem. For continued observation of exudation, it was necessary to remove further petiole or stem slices of about 1 to 10 mm when the exudation became slow or stopped. This is the normal procedure used for such observations. Illumination was enhanced with fiber optic light sources (KL1500, Leica, Germany), adjusted for maximum contrast to facilitate identification of phloem tissues.

The detailed phloem structure was observed with alkaline decolorized aniline blue (DAB) staining of callose using a fluorescence microscope (BX41, Olympus, Japan) under UV excitation with UV filter cube (Model: U-M41012, migrated from Olympus AX70 microscopy system; excitation filter: 330-385 nm, barrier filter: 420 nm). DAB was prepared as 0.01 to 0.5% w/v solutions (pH 8.5) by dissolving its ammonium salt (Sigma) in 10mM Na_2HPO_4 buffer. Free-hand sections were immersed in DAB solution for approximately one minute and mounted in water for observation For cut petiole and stem surfaces, DAB-wetted tissue paper was used to gently touch the surface, followed by observation under UV with UV filter set.

For the phloem tracer experiments, carboxyfluorescein-5(6) (CF-5(6)) was prepared according to (1) and used according to (2). We used CF-5(6) in preference to the diacetate form, because there was no noticeable difference in phloem exudate or phloem tissue labeling patterns between the two forms and because the former was more cost-effective in terms of the large amount necessary to replicate the experiments. CF-5(6) was applied to the leaf surface for 1-2 hours before plants were transported to the microscopy laboratory for observation. CF-5(6) was applied to stem or petiole surfaces for an overnight incubation prior to microscopy analysis, which is when CF-5(6)

signals in exudates were strong enough for photographing. A GFP filter set (excitation filter: 480 ± 20 nm, barrier filter >510 nm) was used to visualize CF-5(6).

Metabolite analysis.

Sampling. For metabolite profiling and measurement, phloem exudates were collected from fresh tissue, and dissected phloem tissues from freeze-dried, fully developed stem vascular bundles.

Phloem exudates were collected according to (3). Immediately after de-topping plants, the earliest initial exudate was removed by clean tissue paper to avoid possible contamination from either broken cells or unknown sources. The subsequent exudate was collected by pipette and immediately transferred to microcentrifuge tubes containing extraction solvent for phloem exudates as described below.

To sample phloem tissues, stem segments were cut from fully elongated, thick basal internodes and immediately frozen in liquid nitrogen, then freeze-dried (Christ Alpha Loc-1m. Osterode, Germany) for 3 days, and stored at –20 ºC in plastic bags filled with nitrogen. The plastic bag was placed in a desiccator with silica gel desiccant until use. Prior to extraction, the entire desiccator was taken out of –20 ºC, filled with nitrogen, and warmed to room temperature before opening the plastic bag. Since the dissection procedure is lengthy, the stem segments were kept in other smaller desiccators in the microscopy lab until immediately before dissection.

Dissection. Double-layered facemasks were worn during the dissecting process to avoid introduction of breath moisture to the desiccated phloem tissues being dissected. Dried stems were cut to 1-2 cm lengths, then sliced longitudinally to leave one or two vascular bundles intact for further dissection. The microscope stage was covered with clean wax-paper backing from Parafilm®, which facilitated the identification of any

contaminating fibers and kept the workspace clean. The following dissection procedure required extreme care at all stages: 1) each cut was done with a new clean razor blade or new blade position; 2) any area that contained visible fibers on the wax-paper backing was removed immediately (or vascular bundles being dissected were removed) and the wax-paper backing was replaced; and 3) clean syringe needles and small forceps were used for handling vascular bundles and dissected phloem tissues.

The square shape of the external phloem facilitates cutting down its four longitudinal sides along its borders to leave only the external fascicular phloem region. Note that it is difficult to obtain perfect cuts in a controlled manner and that imperfect cuts invading adjacent tissues resulted in samples that were not useful for further dissection and were therefore discarded. Unsatisfactory, imprecise dissections were discerned by the different colors, shapes and sizes of cells of the fascicular phloem. Mature (secondary) sieve elements in the fascicular phloem are large and readily identified amongst surrounding cells without staining. The white plug material on sieve plates and white crystal material in sieve elements are also good indicators. After successful dissection, both ends of the dissected fascicular phloem were re-cut to remove any potential contamination acquired during the original cutting of the stem segments. The dissected fascicular phloem tissues were photographed (along the length and from both ends) for subsequent volume estimation (see below). Samples were then transferred to individual microcentrifuge tubes and stored immediately in liquid nitrogen. Both removed ends were then stained with DAB solution for visualizing possible contamination from an unsuccessful cut, and were discarded after observation and photographing. If contamination was detected, the sample was discarded.

Xylem tissue and internal fascicular phloem dissection was also performed similarly. However, the latter is mostly curved shaped and more fragile due to its smaller size,

which greatly reduced the success rate, such that data from only two internal fascicular phloem samples are reported here.

Estimation of dissected tissue volumes and phloem sieve element percentage. The volume of dissected tissues and the percentage by volume of sieve elements in dissected phloem tissues were estimated by analyzing microscopic images of dissected tissues with MetaMorph® offline (version 4.6r9, Universal Imaging Corp., PA, USA). The areas of both ends were estimated by MetaMorph software. Since dissected tissues are close to an elongated cuboid shape, the length of the dissected tissue was multiplied by the average area of both ends to obtain the estimated tissue volume.

To estimate the proportion of sieve elements in dissected fascicular phloem tissues, freeze-dried, un-dissected stem segments were stained with DAB and photographed by UV microscopy. Sieve element regions were selected and their area calculated by MetaMorph® software. The ratio of sieve element area to the total area for counting sieve elements was used to estimate the volume ratio of sieve elements in the total fascicular phloem tissue. Around 45% of the total cross sectional area of the fascicular phloem comprised sieve elements and companion cells (SE/CCC).

Analytical procedure for metabolite analysis. Metabolite profiling and identification from both phloem exudates and dissected tissues were done according to (3-5). For metabolite extraction from exudate, 1 μL of phloem exudate was extracted with water and chloroform (400 μL : 300 μL) and vortexed briefly. After centrifugation at 15,800 x g for 2 minutes, the polar (upper) phase was aliquoted into two parts, one for GC/MS and the other for LC/MS analysis. Metabolite extraction from dissected tissues was processed as described in (6), except that homogenization steps were omitted. To avoid possible sample loss during processing, sample presence in the microcentrifuge tube was visibly confirmed both before and after adding extraction solvents. Aliquots for GC/MS were lyophilized and processed exactly as described in (3). LC-MS analysis was performed as in (4).

Protein composition analysis.

Sampling. For protein analysis, phloem exudates were collected into empty polypropylene centrifuge tubes and stored at -80 °C. 10 mM DTT was added to inhibit gelling, which otherwise impairs re-sampling. One to 2 µL of phloem exudate was used for gel analysis. About 50-100 µg of phloem exudate proteins was loaded onto the gels.

For dissecting phloem tissues, frozen stems stored at -80 °C were partially thawed at 4°C. The vascular bundle was incised through the xylem into two parts. The xylem was then removed and the external phloem strands were stripped out by forceps. Phloem strands of up to a few centimeters from a single vascular bundle can be sampled this way. For internal phloem tissues, xylem was first removed and then visible pith, as judged by the naked eye, was removed by razor blade. Because these samples were for control purposes only, we did not further improve this technique for obtaining a larger amount of pure phloem tissue, as the needle-tip sampling approach (described below) proved more practical. Two to three dissected phloem vascular bundles (2-3 cm in length) were used for each protein extraction.

To sample relatively pure phloem proteins by needle-tip, frozen stems were partially thawed at 4 °C and cut transversely with a razor blade into segments a few millimeters in thickness. Segments were immediately immersed for 1-5 minutes in ice-cold 0.1% (w/v) amido black in 10 mM EDTA (pH ~6.8) for visualizing the phloem proteins, then washed briefly with 10 mM EDTA (pH 6.8) and stored on ice during dissection.

Under the stereomicroscope, the stained fascicular phloem proteins in large sieve elements were readily visible as blue strands of phloem protein aggregate in the longitudinal sections. As the staining procedure does not utilize fixatives, the aggregates retained their elasticity and stickiness and could thus be readily picked up with syringe needle tips for sampling. The needle tip was then dipped into a water solution

containing ice-cold 10 mM EDTA (pH 8.0) in a microcentrifuge tube. Fascicular phloem proteins from ~20 stem sections were sampled in this way and pooled as one sample (of 50-90 µg).

Analytical procedure for protein analysis. For proteins from dissected fascicular phloem tissues, samples were frozen in liquid nitrogen, homogenized to a fine powder and then extracted by phenol (7). Protein samples collected from fascicular phloem tissue by needle tip were processed either by direct acetone precipitation or phenol extraction (7). Phloem exudate protein samples were processed in the same way in parallel. Extracted proteins were analyzed by 1D SDS-PAGE according to (8) or 2D gel electrophoresis according to standard procedures. For 1D gel analysis 0.75-1 cm thick 10% SDS-PAGE were used. Replicates of samples for 1D gel analysis are as follow:

1) Needle-dissected fascicular phloem aggregates: 4 replicates

2) Total external phloem tissues: 4 replicates

3) Phloem exudates: 3 replicates

4) Total internal fascicular phloem tissues: 2 replicates

For 2D gels, samples were suspended in 100 µL sample buffer and all (50-90 µg) was loaded onto a pH 3-10 non-linear strip for IEF. 8-16% gradient gels were used for the second dimensional separation by SDS-PAGE (refer to (9) for detailed procedure on 2-D gel analysis including IEF focusing, SDS-PAGE, gel staining and imaging, spot picking and trypsin digestion procedure). Protein bands or spots from the needle-dissected samples were excised from the gels, digested with trypsin according to standard procedures, then analyzed by nano-LC-ESI-MS/MS. Two replicates were

performed for 2D gel analysis for sampled fascicular phloem aggregates and phloem exudates.

One replicate of needle-dissected fascicular phloem aggregates was used for direct trypsin digest without gel electrophoresis separation. The trypsin-digest of needle-dissected fascicular phloem aggregates was loaded onto a nano-LC-ESI-MS/MS.

Nano-LC was performed with an Eksigent 2D nano-LC system (Dublin, CA, USA) equipped with a Dionex C18 PepMap100 column (75 µm i.d.) (Sunnyvale, CA, USA) flowing at 180 nL/min. Peptides (5 µL injections) were resolved on a gradient that started at 95% solvent A (5% acetonitrile, 0.1% formic acid) and 5% solvent B (95% acetonitrile, 0.075% formic acid in MilliQ water) for 3 minutes, then increasing from 5-25% B over 5 minutes, from 25-60% B over the next 32 minutes, and from 60-95% B over the final 5 minutes. Mass spectrometric analysis was performed on an ABI QSTAR XL (Applied Biosystems/MDS Sciex) hybrid QTOF MS/MS mass spectrometer equipped with a nanoelectrospray source (Protana XYZ manipulator). Positive mode nanoelectrospray was generated from fused-silica PicoTip emitters with a 10 µm aperture (New Objective, Woburn, MA, USA) at 2.5 kV. The m/z response of the instrument was calibrated daily with manufacturer standards. TOF mass and product ion spectra were acquired using information dependent data acquisition (IDA) in Analyst QS v1.1 with the following parameters: mass ranges for TOF MS and MS/MS were m/z 300-2000 and 70-2000, respectively. Every second, a TOF MS precursor ion spectrum was accumulated, followed by three product ion spectra, each for 3 s. The switching from TOF MS to MS/MS is triggered by the mass range of peptides (m/z 300-2000),

precursor charge state (2-4) and ion intensity (>50 counts). The DP, DP2, and FP settings were 60, 10, and 230, respectively, and rolling collision energy was used.

Mascot database searching was according to standard procedures (9) and *de novo* sequencing was conducted with methods reported by (8). Two databases were used for initial database searches 1) non-redundant protein sequence database; 2) EST and Unigene sequences from cucumber (version 1) , melon (version 1) and watermelon (version 1)(http://www.icugi.org). Peptides were also TBLASTN searched against the cucumber genome (10) and BLASTP searched against the pumpkin sap proteome (11). Multiple sequence alignments were generated by ClustalW2 (12).

References

1. Knoblauch M, van Bel AJE (1998) Sieve tubes in action. *Plant Cell* 10(1):35-50.
2. Grignon N, Touraine B, Durand M (1989) 6(5)Carboxyfluorescein as a tracer of phloem sap translocation. *Am J Bot* 76(6):871-877.
3. Fiehn O (2003) Metabolic networks of *Cucurbita maxima* phloem. *Phytochemistry* 62(6):875-886.
4. Tolstikov VV, Fiehn O (2002) Analysis of highly polar compounds of plant origin: Combination of hydrophilic interaction chromatography and electrospray ion trap mass spectrometry. *Anal Biochem* 301(2):298-307.
5. Tolstikov VV, Fiehn O, Tanaka N (2007) Application of liquid chromatography-mass spectrometry analysis in metabolomics. *Metabolomics: Methods and Protocols,* Methods in Molecular Biology (Vol.358), (The Humana Press Inc., Totowa, NJ, USA), pp 141-155.
6. Fiehn O (2006) Metabolite profiling in Arabidopsis. *Arabidopsis Protocols*, Methods in Molecular Biology *(*Vol. 323):439-447.
7. Hurkman WJ, Tanaka CK (1986) Solubilization of plant membrane proteins for analysis by two-dimensional gel electrophoresis. *Plant Physiol* 81:802-806.
8. Walz C, Juenger M, Schad M, Kehr J (2002) Evidence for the presence and activity of a complete antioxidant defence system in mature sieve tubes. *Plant J.* 31(2):189-197.
9. Alvarez S*, et al.* (2009) Comprehensive analysis of the *Brassica juncea* root proteome in response to cadmium exposure by complementary proteomic approaches. *Proteomics* 9(9):2419-2431.
10. Huang S*, et al.* (2009) The genome of the cucumber, *Cucumis sativus* L. *Nature genetics* 41(12):1275-1281.
11. Lin MK, Lee YJ, Lough TJ, Phinney BS, Lucas WJ (2009) Analysis of the pumpkin phloem proteome provides insights into angiosperm sieve tube function. *Mol Cell Proteomics* 8(2):343-356.
12. Thompson JD, Gibson TJ, Higgins DG (2002) Multiple sequence alignment using ClustalW and ClustalX. *Current protocols in bioinformatics* (John Wiley & Sons, Inc., Hoboken, NJ), ed. Baxevanis AD et al, Chapter 2:Unit 2.3.